Electron and Hole Transfer Induced by Thermal Annealing of Crystalline DNA X-Irradiated at 4 K

Michael G. Debije and William A. Bernhard*

Department of Biochemistry and Biophysics, University of Rochester, Rochester, New York 14642

Received: March 15, 2000; In Final Form: May 30, 2000

Recent models for long range (>2 nm) transfer of electrons and holes through DNA suggest a mechanism that is neither a single long distance tunneling event nor a mechanism strictly due to hopping, but a mixture of the two. From results reported here we argue that any complete model of electron or hole transfer in DNA should include the effects of reversible proton transfer. Reversible proton transfer (primarily between guanine-cytosine base pairs) influences the ability of DNA to trap free radicals, which in turn affects the migration of holes and electrons. We present the annealing characteristics of electrons and holes trapped in crystalline oligodeoxynucleotides irradiated at 4 K and annealed stepwise to room temperature (RT). The annealing profiles are relatively insensitive to DNA conformation, sequence, or base stacking continuity. The packing of the DNA duplexes is known, and it is readily shown that electron and/or hole transfer must be intermolecular. The distances required for tunneling between separate molecules are found to be comparable to the distances required for tunneling within a DNA duplex. The annealing characteristics of DNA are considerably different than those found in crystals of α-Me-mannoside, 5′dCMP, and 1-Methylcytosine:5-Fluorouracil. This difference is ascribed to a mechanism wherein reversible proton transfer is a rate-limiting step for electron/hole transfer. Reversible proton transfer is, thereby, a "gate" for electron/hole transfer (via tunneling). Because reversible proton transfer is thermally activated, it is proposed that the energetics of this transfer is a dominant factor in determining the thermal annealing profile of DNA. The competing reactions that govern electron/hole migration created by annealing samples irradiated at 4 K are applicable to electron/hole migration at RT. Evidence for this comes from the observation that, in a number of DNA crystals, the free radical species and radical yields are very similar to crystals irradiated at RT compared to those irradiated at 4 K followed by annealing to RT. The proposed mechanism for electron and hole migration through DNA is one where short transfers (∼≤1 nm) occur by tunneling, and tunneling is gated by reversible proton-transfer.

Introduction

Previous work in our lab has demonstrated that crystalline DNA at 4 K is an excellent scavenger of free radicals, trapping on the order of 60% of the holes and electrons created by a radiation track. The total number of radicals trapped by DNA appears to be relatively independent of the conformation, sequence, base stacking continuity, hydration, and counterion of the sample, and primarily a function of the density of packing.[1−3]

It has been known for decades that DNA irradiated at low temperatures and subsequently annealed exhibits a decrease in the population of DNA trapped radicals. This loss is primarily due to combination events between holes and electrons. The final radical population at room temperature is one in which excess electrons or holes have encountered deep potential wells where they are trapped, often by irreversible protonation or deprotonation reactions. The process by which DNA loses free radicals is thermally activated. The probability of a combination event is related to the probability of a hole and/or electron escaping its potential well, migrating between bases, and then encountering a charge partner. This type of thermally driven charge migration has been described by others (see for example Razskazovskiy et al.[4]).

We favor the view that transfer of holes and electrons is neither a single-step long-range tunnel nor adjacent base hopping, but rather a mixture of the two.[5] Recent work has suggested hole transfer is a series of 'hopping' events with short tunneling steps over 2 or 3 intervening base pairs.[6−8] Schuster's group suggests a phonon-assisted polaron model that involves local distortions of the helix.[9,10] Our model for hole and electron transfer has been published previously.[11] The essential element of our hypothesis dictates that electron and hole tunneling along the π-bonded orbitals of the base stack, between strands in the helix, and between helices are "gated" by reversible proton transfer events (Steenken has previously described the trapping of holes and electrons by reversible proton transfer[12−14]). We present here the results of thermal annealing as evidence in support of this model. The possibility that electron and hole transfer is gated by proton transfer has been suggested in passing by others[8,9] but has not actually been incorporated into the description of charge migration in DNA.

The upper limit of the rate of hole hopping measured by Lewis et al.[15] is a factor of 10 slower than the predicted rate.[8] The rate for electron transfer is comparable to that of hole transfer (see ref 16 for a recent review). The rate of proton transfer between bases could be on the order of a molecular vibration and so should be competitive with charge transfer.[14] Inclusion of this reversible proton transfer gating mechanism into the scheme of electron and hole transfer in DNA is likely

* To whom correspondence should be addressed. E-mail: William_Bernhard@urmc.rochester.edu. Fax: (716) 275-6007. Phone: (716) 275-3730.

10.1021/jp000988j CCC: $19.00
Published on Web 07/21/2000

TABLE 1: Crystal Structure, Free Radical Yields, and Annealing Characteristics

oligodeoxy nucleotide sequence	conformation	stacking continuity[a]	free radical yield using 4 K irradiation (μmol/J)	% radical concentration remaining using 4 K irradiation followed by RT anneal	radical yield using RT irradiation (μmol/J)	ref
CTCTCGAGAG	B	Y	0.70 ± 0.06[b]			54
CGCGAATTCGCG	B	N	0.66 ± 0.06[b]	5	0.2[d]	53
CCAACGTTGG	B	Y	0.78 ± 0.05	1	0.1[d]	55
CTCGAG	B	Y	0.75 ± 0.14[c]	5		56
GCGGGCCCGC (I)	A	N	0.55 ± 0.10[b]	17	0.03[d]	57
GCGGGCCCGC (II)	A	N	0.58 ± 0.08[b]	2	0.02[d]	57
GCACGCGTGC	A	N	0.57 ± 0.04[b]	6	0	58
GTGCGCAC	A	N	0.72 ± 0.07[b]	15	0.1[d]	59
CCCTAGGG	A	N	0.70 ± 0.04[c]	4	0	60
CACGCG:GTGCGC	Z	Y	0.61 ± 0.03[b]			61
CGCACG:GCGTGC	Z	Y	n/a	3	0.025[d]	61
CGCGCG (I)	Z	Y	0.73 ± 0.10[b]	11		62
CGCGCG (II)	Z	Y	0.70 ± 0.06[b]			63
CGCGCG (III)	Z	Y	0.57 ± 0.05[b]			64
CGCG	Z	Y	0.65 ±0.15[b]	18	0.14	65
α-Me-mannoside	-	-	0.44 ±0.03[c]	26		66
5′dCMP	-	-	<0.01[e]	15		67
1-MeC:5-F-U	-	-	0.038 ±0.009	0		43

[a] "Y" indicates that the helices are continuously stacked in the crystal, while "N" signifies that they are not. [b] Reference 2. [c] Reference 1. [d] Estimated minimum yield from a single measurement. The contribution from quartz was subtracted prior to yield calculation for radicals trapped by DNA. [e] Reference 68.

to explain the current discrepancy between experiment and theory and provide a more complete picture of radical migration through DNA.

Materials and Methods

Oligodeoxynucleotides were purchased from TIB Molbiol, Midland Certified Reagent, and Ransom Hill Bioscience, and used for crystal growth without further purification. For details on crystal growth and preparation see ref 2. The sugar and base-component crystals described in Table 1 were grown following published procedures.

Irradiation of the crystalline samples was done at either 4 K or room temperature with X-rays generated by a Varian/Eimac OEG-76H tungsten-target tube operated at 70 keV and 20 mA in the Janis dewar setup.[17] The dose rate was 26 kGy/h. Free radical yields were measured in the Q-band Varian E-12 electron paramagnetic resonance (EPR) spectrometer by comparing the intensity of the EPR signal at 4 K to that of a ruby standard mounted on the side of the EPR cavity (see refs 2 and 18). All annealed samples received a dose greater than 5 kGy, which is into the saturation region of the dose−response curve.[2]

Anneals were accomplished by raising the sample 40 cm above the cavity to the heater position, where the temperature was maintained to ±3% by a DRC-82 temperature controller from Lake Shore Cryrotronics. The samples were normally kept at the annealing temperature 10 min. The samples were then lowered back into the cavity and allowed to return to 4 K before spectra were again recorded. The estimated error for the relative radical concentration is somewhat smaller than ±0.1 at high radical concentrations and somewhat larger than ±0.1 at low radical concentrations.

Results

The oligodeoxynucleotide crystalline samples were annealed stepwise, with 80 K as the first step and up to room temperature (RT) as the last step. Data for three of the crystalline DNA sequences, each measured by at least six independent experiments, are shown in Figure 1. These annealing profiles are representative of three different conformations: A-, B-, and Z-DNA. The scatter in the data increases as the annealing temperature is increased. We do not believe scatter for any given

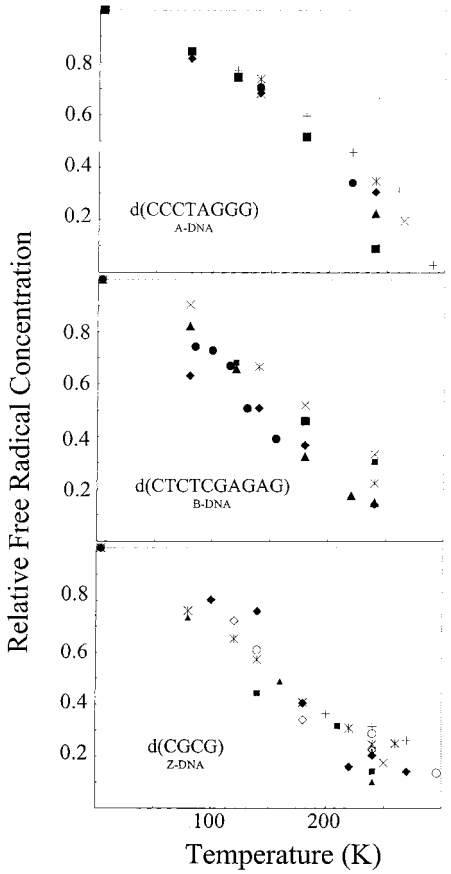

Figure 1. Thermal annealing profiles for (top) seven oligodeoxynucleotide crystalline samples of d(CCCTAGGG), an A-DNA, (middle) six crystalline samples of d(CTCTCGAGAG), a B-DNA, and (bottom) nine crystalline samples of d(CGCG), a Z-DNA. The concentration of radicals after various anneals is plotted along the vertical axis as a fraction of the radicals present at 4 K. There is a ±3% error in the measured temperature. The estimated error for the relative radical concentration is ±0.1; the error is somewhat smaller than this at high radical concentrations and somewhat larger at low radical concentrations.

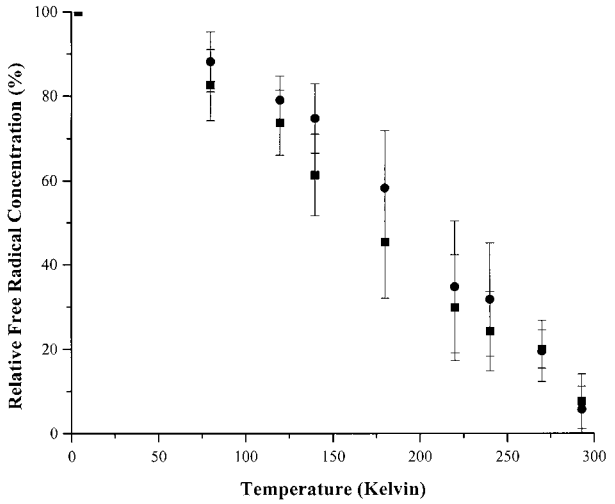

Figure 2. Thermal annealing data comparing DNA crystals with continuous base stacking, squares, and noncontinuous base stacking, circles (see Table 1). Relevant data from a total of 38 crystals with continuous stacking were averaged at each annealing temperature. For noncontinuous stacking, data from 43 crystals was averaged. Samples of every oligodeoxynucleotide sequence shown in the Table are represented.

crystal type is due to variability in purity or crystallinity of the sample. The increased scatter is due primarily to other factors: accuracy of the annealing temperature, variability in the annealing rate, and predominantly the decreased signal-to-noise due to broader and weaker EPR spectra of the annealed sample. The latter leads to increased integration errors.

From Figure 1 and Table 1, there is little difference between conformational types in the fractional number of radicals lost when DNA is annealed to 240 K. On average the Z-DNA crystals lost 76% of the initial radical population, the B-DNA crystals lost 71%, and the A-DNA crystals lost 72%. Generally, base stacking in Z-DNA has an axial rise of ~0.37 nm with a base pair tilt of 9° with respect to the vertical helical axis, B-DNA has an axial rise of 0.34 nm with a 1° tilt, and A-DNA displays an axial rise of ~0.26 nm and a 19° tilt.[19] Neither the change of separation distance of the base planes nor degree of π-overlap between bases had a large effect on the degree to which radicals were lost by combination reactions.

A plot comparing the averaged annealing properties of fifteen oligonucleotide sequences grouped by their stacking continuity is shown in Figure 2. Continuous stacking refers to crystals in which the terminal base pair of one helix abuts the first base pair of the next helix, maintaining π-bonding overlap. In the noncontinuously stacked DNA, the terminal base pairs jut into the side groove of its neighbor, and there is no continuity in the π-bonding system between adjacent oligodeoxynucleotide duplexes.

DNA crystal annealing characteristics were compared with annealing profiles of three other crystalline systems shown in Figure 3: α-Me-mannoside, 5′dCMP, and 1-Methylcytosine: 5-Fluorouracil (1-MeC:5-FU).

A comparison of the quantitative and qualitative differences between crystalline oligodeoxynucleotide samples irradiated cold then annealed to RT and the same oligodeoxynucleotides irradiated at RT was made. The free radical yield for RT irradiated d(CGCG) was G ≈ 0.14 ± 0.04 μmol/J. Yields estimated from single data points for several other oligodeoxynucleotide crystal sequences irradiated at room temperature are shown in Table 1. A comparison of the spectra for two systems, d(CGCACG:GCGTGC) and d(CCCTAGGG) irradiated at 4 K

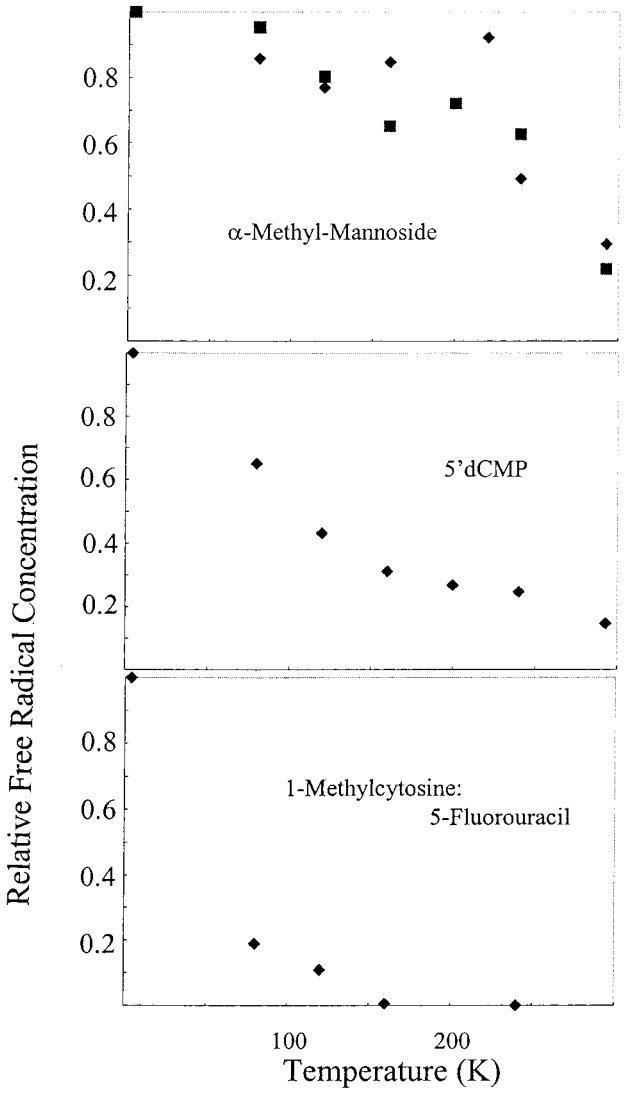

Figure 3. Thermal annealing profiles of (a) α-Me-mannoside, (b) 5′dCMP, and (c) 1-Methylcytosine: 5-Fluorouracil (1-MeC:5-FU). The concentration of radicals after various anneals is plotted along the vertical axis as a fraction of the radicals present at 4 K. There is a ±3% error in the measured temperature. The estimated error for the relative radical concentration is ±0.1; the error is somewhat smaller than this at high radical concentrations and somewhat larger at low radical concentrations.

followed by an anneal to RT, and the same oligodeoxynucleotide irradiated RT are shown in Figure 4a,b. The comparison is hampered somewhat by variable amounts of background signal due to the quartz sample tube. This background becomes a significant factor in spectra that are relatively weak because annealing reduces intensity by an order of magnitude or more, and gives broader spectra. As may be seen in Figure 4a, besides the differences due to the quartz background, there is little difference in the radical species making up the spectra of the two samples. However, the RT irradiated and annealed spectra of d(CCCTAGGG) differ markedly with respect to intensity; radical yields are effectively zero after RT irradiation and of course no comparison can be made of radical types (Figure 4b).

Discussion

Previous work has demonstrated that holes transfer between the two strands of a DNA helix, i.e., transfer is not just intrastrand but also interstrand.[6,7,10,20] Our results demonstrate that hole and/or electron transfer is also intermolecular, occurring even in the absence of base stacking.

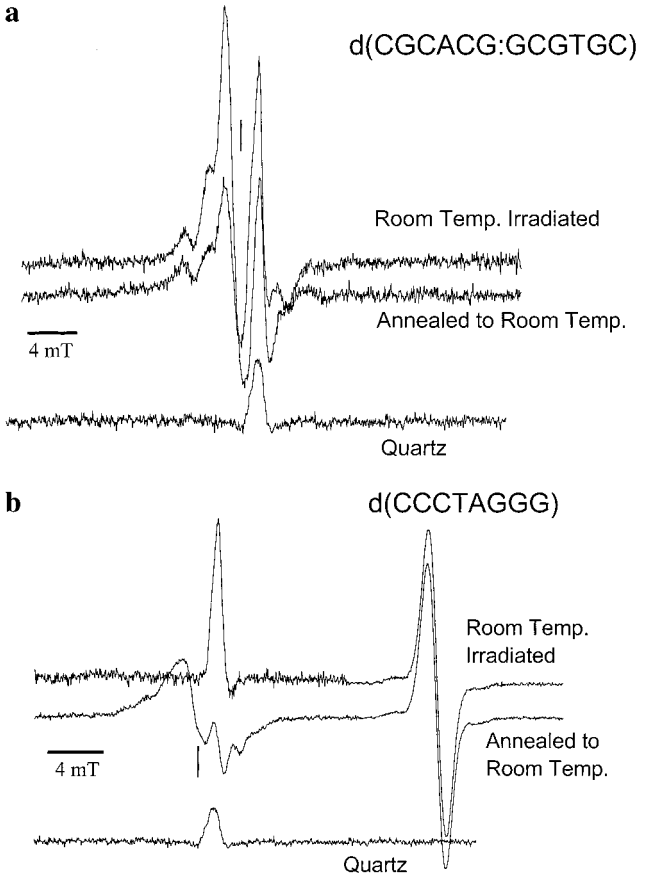

Figure 4. (a) EPR spectra of d(CGCACG:GCGTGC) recorded at 4 K with a spectral width of 40 mT. The room-temperature irradiated sample weighed 278 μg and was irradiated to a dose of 13 kGy. The room-temperature annealed sample weighed 303 μg and was measured at the same gain after a 26 kGy irradiation. The quartz sample was irradiated at 4 K and annealed to RT, and is provided as a reference. The vertical line corresponds to the position of $g = 2.0022$. (b) EPR spectra of d(CCCTAGGG) recorded at 4 K with a spectral width of 40 mT; this scan includes the strong singlet of the ruby reference at high field. The vertical line corresponds to the position of $g = 2.0024$. There is no apparent signal from the DNA sample; the spectrum is dominated by the quartz signal arising from the quartz tube containing the DNA. This can be seen by comparison with the quartz tube signal shown at the bottom. The room-temperature irradiated sample weighed 707 μg and the sample was irradiated to a dose of 13 kGy. The room-temperature annealed sample weighed 624 μg and is at the same gain after a 26 kGy irradiation.

The conclusion that electron/hole transfer is intermolecular in these crystalline samples hinges on the observation that the probability of trapping more than one radical in a single oligodeoxynucleotide duplex is vanishingly small. This is because the distances between trapped radicals are large compared to the length of the DNA duplex (even at dose saturation where the highest possible radical concentrations are obtained). The lengths of the oligodeoxynucleotides listed in Table 1 vary from 4 to 12 base pairs (bp). Each duplex occupies a cylindrical volume of roughly 2.0 nm in diameter and 1.4−4.1 nm in length. For the samples used in annealing, the average separation between radicals was greater than 25−40 nm, corresponding to 70−120 bp. Furthermore, no radical pairs (two radicals close enough to result in electron−electron dipolar coupling) were detected, which means that most (>90%) of the radicals are separated by at least 1−3 bp (0.5−1 nm). It follows that any significant (>5%) reduction in free radical concentration requires that electrons and/or holes transfer between separate molecules. Even at temperatures below 80 K, the observed radical combination reactions must entail intermolecular electron/hole transfer.

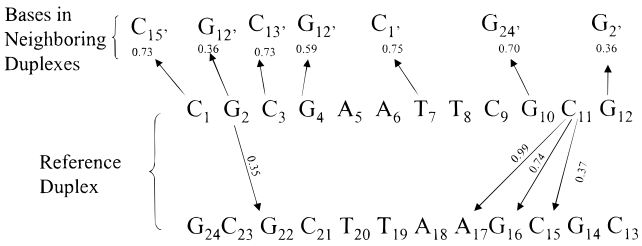

Figure 5. Tunneling distances for the d(CGCGAATTCGCG) crystal were determined from the crystal structure.[53] The distances, in nm, are between bases within the reference duplex and between bases in the reference duplex and neighbor molecules. The primed subscripts indicate bases in neighbor molecules. For hole transfer, guanine−guanine distances (only) were determined, and for electron transfer cytosine/thymine to cytosine/thymine distances (only) were determined. All distances are closest approach between two atoms in the aromatic ring of the bases; exocyclic atoms were excluded.

TABLE 2: Interhelical Base Separation As Measured by the Distance between the Two Closest Ring Atoms on Separate Bases

sequence	minimum G to G distance (nm)	minimum C/T to C/T distance (nm)
CGCGCG	0.497	0.963
CTCTCGAGAG	0.813	>1.0
CGCGAATTCGCG	0.357	0.729
GTGCGCAC	0.435	0.442
CCCTAGGG	0.571	0.535
GCGGGCCCGC (I)	0.404	0.643
GCGGGCCCGC (II)	0.365	0.595
GCACGCGTGC	0.344	0.589

The through-space distances involved in intermolecular transfer are on the order of base-pair separation distances within the DNA duplex. Consider Figure 5, a representation of tunneling distances required for guanine-to-guanine hole transfer and cytosine/thymine-to-cytosine/thymine electron transfer in the d(CGCGAATTCGCG) crystal. The base stacking is discontinuous in this crystal. These base-to-base distances were chosen because it has been shown that the primary trapping site for the hole is on guanine, and for the electron is on the pyrimidines, either cytosine or thymine.[21−30] These distances, therefore, reflect separations between sites that are most likely to be involved in transfers between adjacent molecules. The distances were measured using the crystal structure from the Protein Data Bank,[31] considering only the closest base ring atom to base ring atom. If exocyclic groups are considered, these distances are generally shorter. A summary of minimum intermolecular transfer distances for several other oligodeoxynucleotide crystals are provided in Table 2. The intermolecular distances are comparable to intramolecular distances; for example, hole transfer along a GXGXGX strand (X ≠ G) entails a 0.68 nm distance in B-DNA.[7] That holes and electrons transfer between molecules via tunneling is reasonable given the intermolecular distances found in DNA crystals, the dependence of tunneling rate on distance measured by others,[32−34] and the long time (minutes) between measurements.

Figures 1 and 2 show that radical combination in crystalline DNA is thermally activated throughout the annealing range of 80 to 295 K. This wide range of temperatures is indicative of a wide dispersion in activation energies. The annealing properties of the crystalline DNA are relatively independent of the conformation, base sequence, and base stacking of the helices, which indicates these properties are not the primary determinants of the dispersion. As to what the primary factors might be, we

consider three: nonhomogeneous inter-radical spacing, thermal properties of the lattice, and proton transfer.

Given the short migration distances of electrons and holes in DNA at 4 K and the related high trapping efficiency, the spatial distribution of trapped radicals will retain some degree of the nonhomogeneous spacing that is inherent in the energy deposition track.[35−37] If the charge created by ionization remains in close proximity to the unpaired electron, there exists a strong Coulombic influence for radical recombination. Since the spacing between radicals is variable, this will create dispersion in activation energies related to inter-radical spacing, with closely spaced radicals having relatively lower activation energies. However, if this were a major factor, the crystals of α-Me-mannoside (Figure 3), which have radical concentrations comparable to DNA, should reflect this Coulombic influence with a similar annealing profile, but it does not. While some of the dispersion in the DNA crystals must be related to nonhomogeneous radical spacing, this is not a major determinant of the annealing profile.

It would seem that the thermal properties of the lattice could have a significant influence on the annealing profiles. Phonon activated polaron transfer, as described by Schuster,[9,10] is an attractive model for hole and electron transfer in DNA. Thermal excitation of lattice modes allows for excitation of the radical from its trapped state. One might expect, therefore, that changes in the lattice could have pronounced effects on the annealing profiles. For example, the annealing profiles observed for α-Me-mannoside, 1-MeC:5-FU, and 5′dCMP are quite distinct from each other and from DNA crystals. These three crystals have relatively simple lattices compared to the lattices of DNA. Since the DNA crystals are more likely to contain disordered molecules (primarily solvent) and lattice defects, this could be a factor behind the large dispersion in activation energies. But it is unlikely to be the dominant factor because within the group of DNA crystals studied there is a considerable diversity in lattice structures. For example, the d(CACGCG:GTGCGC) crystal is highly ordered. It diffracts to 1.6 Å resolution and the position of most of the waters (3.5 out of a calculated 4.2 waters per nucleotide) are well determined. In comparison, the d(GCGGGCCCGC) (II) crystal is less well ordered. It diffracts to 1.8 Å and only a small fraction of the water molecules (3.8 out of a calculated 15.6 waters per nucleotide) are ordered. Yet, these two crystals have almost the same annealing profile.

Furthermore, the annealing curves for DNA powders[29,38,39] and films (Milano, unpublished results) are very similar to those of DNA crystals. In contrast, the α-Me-mannoside and 5′dCMP have similar lattice structures but very different annealing profiles. It is unlikely, therefore, that the annealing profiles can be explained by lattice properties alone; there must be other major determinants. We suggest a model where reversible proton transfer plays a major role in modulating electron/hole migration.

The trapping and de-trapping of both electrons and holes in protic systems such as DNA depends on the competition between proton transfer and electron/hole transfer.[14] Localization of migrating holes or electrons on bases creates sizable changes in the relative acidity and basicity of those bases. These changes create a driving force for reversible proton transfer across specific base pair hydrogen bonds. The driving force is positive for deprotonation of the guanine radical cation and for protonation of the cytosine radical anion. Proton transfer leads to a 0.52 eV (50 kJ/mol) increase in the electron affinity of cytosine and a 0.54 eV (52 kJ/mol) decrease in the ionization energy of guanine. The transfer of a proton to $C^{\bullet-}$ from guanine has a $\Delta G \leq -20$ kJ/mol.[13,24] The transfer of a proton to a base partner

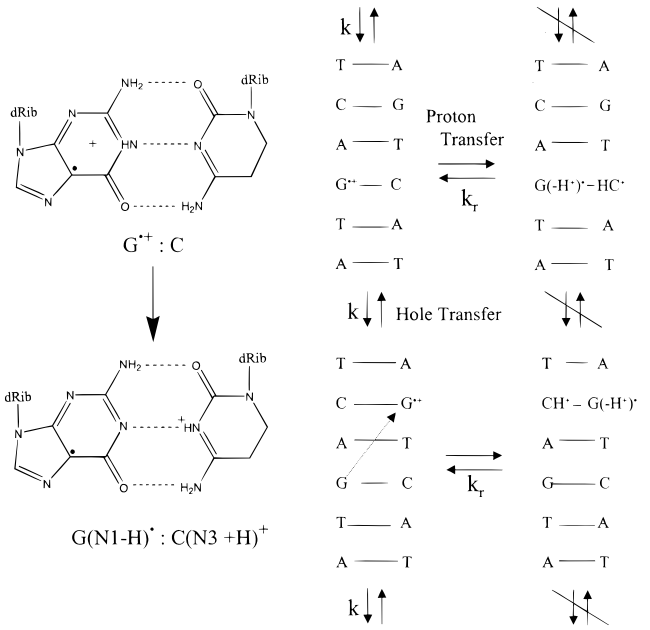

Figure 6. Reversible proton transfer and its influence on the migration of the hole. In this example, a hole resides on guanine. The increased acidity of the oxidized guanine promotes an energetically favorable proton transfer to cytosine, forming $G(N1-H)^{\bullet}$:$C(N3+H)^{+}$, an event that is in competition with hole transfer to another guanine. Deprotonation of the guanine radical cation separates charge from the unpaired electron. Because this trap is energetically deeper, radical migration is slowed and may even halt. Increased thermal energy activates back-transfer of the proton, opening the gate and allowing the hole to migrate from $G^{\bullet+}$ to a nearby G.

results in the stabilization of the unpaired electron as a neutral radical and moves the formal charge to its conjugate base. Subsequent thermal energy permits back-transfer of the proton, and allows the hole or electron to continue its migration by once again creating a mobile charged radical (see Figure 6).

Proton transfer between base-pairs can occur at rates that are competitive with electron and hole transfer. The rate of hole transfer has been predicted by Bixon et al. to be on the order of 10^9 s^{-1},[8] but measured by Lewis et al. to be at most 10^8 s^{-1}.[15] The rate of electron transfer has been less well defined, but has been estimated at up to 10^{12} s^{-1}.[16] Proton transfer between base pairs, in contrast, could occur on the time scale of a single molecular vibration of 10^{14} s^{-1} at the upper limit.[14]

We propose the difference between the measured and predicted rates of hole transfer could be explained by including a reversible proton-transfer rate. We propose a radical transfer model where electron/hole transfer, at a rate k, competes with reversible protonation/deprotonation of rate k_r, and also competes with irreversible reactions of rate k_i (see Scheme 1). One example of an irreversible reaction is proton transfer to C6 of the thymine radical anion.[29,40] Another example is hydroxide addition to C8 of the guanine radical cation.[41] This particular reaction, however, appears to depend strongly on the DNA being in double strand form; if it is in single strand or monomer form, other reactions dominate, such as hydrogen abstraction from the deoxyribose moiety.[42] These irreversible reactions terminate electron/hole migration. The reversible reactions impede migration but do not necessarily stop it, depending on the temperature and activation energy. The migration of the hole or electron via short tunneling events is thus "gated" by reversible proton transfer.

To support such a model, we consider the annealing profiles of the three crystalline compounds shown in Figure 3. These

SCHEME 1: Kinetic Scheme for Electron/Hole Transfer[a]

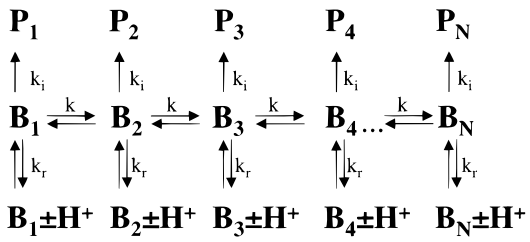

[a] B stands for a base, $B\pm H^+$ represents a reversible protonation/deprotonation event, and P represents products formed by irreversible reactions (including irreversible protonation/deprotonation). The activation energy required for P formation is significantly larger than that needed for $B\pm H^+$ formation; thus, at low temperatures migration occurs in the absence of P formation. But if the temperature is too low, $B\pm H^+$ formation blocks migration.

were chosen because the hydrogen bonding schemes are such that reversible proton-transfer is not expected to be as facile as it is in DNA. The 1-MeC:5-FU crystal has stacked molecular planes separated by 0.298 nm with little overlap of π orbitals between adjacent levels.[43] Within each plane, 1-MeC forms a hydrogen-bonded pair with 5-FU, and these pairs hydrogen bond with other pairs, forming an extended H-bonded sheet. At 4 K, the yield of trapped radicals in the cocrystal is an order of magnitude below that of DNA (see Table 1). Less than 5% of the radical ions initially formed by the radiation track result in stable free radicals on the bases. Other studies have shown that two major radicals are trapped in the 1-MeC:5-FU crystal: the oxidation product is the N1 deprotonated radical cation of uracil (5FU(N1−H)•) and the reduction product is the N3 protonated radical anion of 1-MeC (MeC(N3+H)•).[44,45] Therefore, trapping of two dominant radical species, although inefficient, is accompanied by reversible proton transfer. The annealing profile shows a quick drop in radical population at low temperature, consistent with a small activation energy that is relatively well-defined. This cocrystal illustrates three important points. 1. Because the yield of trapped radicals is low, the migration distance of the electron or hole must be relatively large (in order to explain the high percentage of combination reactions). 2. In protic systems such as DNA and its constituents, radical trapping at <100 K is almost always (perhaps always) accompanied by proton transfer that returns the molecular site to its original charge state.[46] 3. The energy of stabilization, due largely to reversible proton transfer, can be quite small.

The α-Me-mannoside crystal provides a contrasting example. The initial trapped radical yields are high, comparable to DNA,[1] but unlike DNA the radical concentration changes very little (<25%) over the annealing temperature range of 4 K to 200 K. The identity of the radicals and thermally activated reactions throughout this temperature range are well understood,[47,48] (Bernhard, unpublished). At 4 K the two dominant radicals are a trapped electron (analogous to that observed by Box[49]) and a radical formed by the net loss of hydrogen from the methyl group. In addition there are minor amounts of two different alkoxy radicals. Upon warming to 80 K, the trapped electrons have combined completely and accounts for the bulk of the decline in radical concentration seen in Figure 4a. Between 80 and 200 K there are two major reactions that involve internal conversions but no net loss of total radicals. Above 200 K, several additional reactions occur, and the radical concentration drops precipitously. The radical decay in this system is well explained by the migration of the naked electron at lower temperatures and of hydrogen atoms at higher temperatures. This crystal illustrates two important points. (1) In the absence of trapping by *reversible* proton transfer, trapping occurs via *irreversible* proton transfer. The efficiency of the latter can be comparable to the former, i.e., comparable yields in α-Me-mannoside and DNA. (2) De-trapping a radical produced by irreversible proton transfer requires a high activation energy, high enough to promote free radical reactions that are not mediated by electron transfer.

The 5′dCMP annealing curve can be viewed as a composite of that observed for α-Me-mannoside and that of 1-MeC:5-FU. At 6 K the 5′dCMP crystals traps both base and sugar centered radicals.[50,51] The initial loss of radicals upon annealing is similar to the profile of 1-MeC:5-FU in that the base radicals combine quickly as the electrons and holes transfer through the matrix. A large fraction of the remaining radical population consists of sugar-centered radicals that are relatively stable between 100 and 250 K with a drop in the free radical concentration at higher temperatures, similar to the α-Me-mannoside crystal. The 5′dCMP crystal anneals in a manner that combines the response observed for crystals containing just sugar and the 1-MeC:5-FU cocrystal.

We hypothesize that differences in proton transfer are primarily responsible for the difference between the annealing profile of the oligonucleotide crystals and the three other materials presented. It is known that proton transfer occurs in DNA systems over a wide range of temperatures. For the example mentioned above, electrons initially trapped on cytosine at 77 K migrate to thymine upon annealing, where irreversible proton transfer to C6 of one-electron reduced thymine forms the 5,6-dihydrothymine-5-yl radical, T(C6+H)•, at around 180 K.[29,40] The T(C6+H)• radical is stable even at RT; it is a relatively deep electron trap. Other work has demonstrated that proton transfer can occur at low temperatures (<77 K) as well.[40,46,52]

One might ask if the reactions obtained by annealing cold-irradiated crystals to RT are the same as the reactions that occur when crystals are irradiated at RT. The following experiments indicate that they are in some cases, and, perhaps, in most cases. Several oligodeoxynucleotide samples were irradiated at both RT, and at 4 K, the latter samples subsequently annealed to RT. As may be seen from Table 1, for most crystals there was little difference in the free radical yield. In addition, the types of free radical are quite similar for most crystals. As an example, a comparison of the EPR spectra of d(CGCACG:GCGTGC) is shown in Figure 4a. There are exceptions where the free radical yield obtained by RT irradiation is smaller, effectively zero (see Figure 4b for an example). In our working model, these variations can be explained by changes in the relative rates (k, k_r, and k_i) shown in the scheme. There is no compelling reason based on structure or packing to believe that this latter sample has any new or extraordinary room-temperature conductivity. What properties these particular crystals possess that differentiate their ability to trap radicals at RT have not yet been identified.

Our radical trapping and annealing results do NOT support the proposal that π-electron bonding between stacked bases (π-ways) mediate long distance tunneling in DNA. In addition, we believe it is important to design experiments that measure the degree to which reversible proton-transfer competes with hole and electron transfer. It is possible that a major fraction of the polaron trapping energy is accounted for by reversible proton transfer.

Conclusion

The ability of holes and electrons to combine in thermally annealed crystalline DNA samples is relatively independent of

the conformation, sequence, and base stacking of the DNA helices. The migration of holes and electrons through the crystalline DNA lattice requires intermolecular transfer. The distances involved in intermolecular transfers are comparable to distances involved in intramolecular transfers. Additionally, we have given evidence that, in a number of cases, the reaction sequences initiated by 4 K irradiation followed by anneal to room temperature are essentially the same as those initiated by room-temperature irradiation.

Neither the π-stacking in DNA, nor any other of its intramolecular bonding, confers upon DNA the properties expected of a wire (a metal-like conductor). It is suggested that electron and hole migration proceeds via short tunneling steps and that tunneling competes with reversible proton transfer.

Acknowledgment. We thank Michael Strickler for his assistance with the computer structure analysis, Yuriy Razskazovskiy for his helpful discussions, and Kermit R. Mercer for his technical assistance. The investigation was supported by PHS Grant 2-R01-CA32546, awarded by the National Cancer Institute, DHHS. Its contents are solely the responsibility of the authors and do not necessarily represent the official views of the National Cancer Institute.

References and Notes

(1) Debije, M. G.; Milano, M. T.; Bernhard, W. A. *Angew. Chem., Int. Ed. Engl.* **1999**, *38*, 2752−2756.
(2) Debije, M. G.; Bernhard, W. A. *Radiat. Res.* **1999**, *152*, 583−589.
(3) Debije, M. G.; Strickler, M. D.; Bernhard, W. A. *Radiat. Res.* **2000**, *154*, 163−170.
(4) Razskazovskii, Y.; Swarts, S.; Falcone, J.; Taylor, C.; Sevilla, M. *J. Phys. Chem. B* **1997**, *101*, 1460−7.
(5) Jortner, J.; Bixon, M.; Langenbacher, T.; Michel-Beyerle, M. E. *Proc. Natl. Acad. Sci. U.S.A.* **1998**, *95*, 12759−12765.
(6) Meggers, E.; Kusch, D.; Spichty, M.; Wille, U.; Giese, B. *Angew. Chem., Int. Ed. Engl.* **1998**, *37*, 460−462.
(7) Meggers, E.; Michel-Beyerle, M. E.; Giese, B. *J. Am. Chem. Soc.* **1998**, *120*, 12950−12955.
(8) Bixon, M.; Giese, B.; Wessely, S.; Langenbacher, T.; Michel-Bayerle, M. E.; Jortner, J. *Proc. Natl. Acad. Sci. U.S.A.* **1999**, *96*, 11713−11716.
(9) Henderson, P. T.; Jones, D.; Hampikian, G.; Kan, Y.; Schuster, G. B. *Proc. Natl. Acad. Sci. U.S.A.* **1999**, *96*, 8353−8358.
(10) Ly, D.; Sanil, L.; Schuster, G. B. *J. Am. Chem. Soc.* **1999**, *121*, 9400−9410.
(11) Bernhard, W. A.; Debije, M. G.; Milano, M. T.; Razskazovskiy, Y. *Proceedings Eleventh International Congress of Radiation Research*, Vol. 2; Moriarty, M., Mothersill, C., Seymour, C., Edington, M., Ward, J. F., Fry, R. J. M., Eds.; Allen Press Inc.: Lawrence, KS, 2000; pp 321−324.
(12) Steenken, S. *Chem. Rev.* **1989**, *89*, 503−520.
(13) Steenken, S. *Free Rad. Res. Commun.* **1992**, *16*, 349−379.
(14) Steenken, S. *Biol. Chem.* **1997**, *378*, 1293−1297.
(15) Lewis, F. D.; Liu, X.; Miller, S. E.; Wasielewski, M. R. *J. Am. Chem. Soc.* **1999**, *121*, 9746−9747.
(16) Grinstaff, M. W. *Angew. Chem., Int. Ed. Engl.* **1999**, *38*, 3629−3635.
(17) Mercer, K. R.; Bernhard, W. A. *J. Magn. Reson.* **1987**, *74*, 66−71.
(18) Milano, M. T.; Hu, G. G.; Williams, L. D.; Bernhard, W. A. *Radiat. Res.* **1998**, *150*, 101−114.
(19) Saenger, W. *Principles of Nucleic Acid Structure*; Springer-Verlag: New York, 1984.
(20) Giese, B.; Wesseley, S.; Spormann, M.; Lindemann, U.; Meggers, E.; Michel-Beyerle, M. E. *Angew. Chem., Int. Ed. Engl.* **1999**, *38*, 996−998.
(21) Yan, M.; Becker, D.; Summerfield, S.; Renke, P.; Sevilla, M. D. *J. Phys. Chem.* **1992**, *96*, 1983−1989.
(22) Melvin, T.; Cunniffe, S. M. T.; O'Neill, P.; Parker, A. W.; Roldan-Arojna, T. *Nucl. Acids Res.* **1998**, *26*, 4935−4942.
(23) Hüttermann, J.; Voit, K.; Oloff, H.; Köhnlein, W.; Gräslund, A.; Rupprecht, A. *Faraday Discuss. Chem. Soc.* **1984**, *78*, 135−149.
(24) Steenken, S.; Jovanovic, S. V. *J. Am. Chem. Soc.* **1997**, *119*, 617−618.
(25) Cullis, P. M.; Evans, P.; Malone, M. E. *Chem. Commun.* **1996**, 985−986.
(26) Sevilla, M.; Becker, D.; Yan, M.; Summerfield, S. *J. Phys. Chem.* **1991**, *95*, 3409−15.
(27) Bernhard, W. A. *Free Rad. Res. Commun.* **1989**, *6*, 93−94.
(28) Bernhard, W. A. In *The Early Effects of Radiation on DNA*; Fielden, E. M., O'Neill, P., Eds.; Springer-Verlag: Berlin, Heidelberg, 1991; Vol. Ser. H 54, pp 141−54.
(29) Wang, W.; Sevilla, M. *Radiat. Res.* **1994**, *138*, 9−17.
(30) Bernhard, W. A. *J. Phys. Chem.* **1989**, *93*, 2187−2189.
(31) Berman, H. M.; Westbrook, J.; Feng, Z.; Gilliland, G.; Bhat, T. N.; Weissig, H.; Shindyalov, I. N.; Bourne, P. E. *Nucl. Acids Res.* **2000**, *28*, 235−242.
(32) Brun, A. M.; Harriman, A. *J. Am. Chem. Soc.* **1992**, *114*, 3656−3660.
(33) Meade, T. J.; Kayyem, J. F. *Angew. Chem., Int. Ed. Engl.* **1995**, *34*, 352−4.
(34) Lewis, F. D.; Wu, W.; Zhang, Y.; Letsinger, R. L.; Greenfield, S. R.; Wasielewski, M. R. *Science* **1997**, *277*, 673−676.
(35) Mozumder, A.; Magee, J. L. *Radiat. Res.* **1966**, *28*, 203−214.
(36) Paretzke, H. G.; Turner, J. E.; Hamm, R. N.; Ritchie, R. H.; Wright, H. A. *Radiat. Res.* **1991**, *127*, 121−9.
(37) Nikjoo, H.; Uehara, S.; Wilson, W.; Hoshi, M.; Goodhead, D. *Int. J. Radiat. Biol.* **1998**, *73*, 355.
(38) Mroczka, N. E.; Bernhard, W. A. *Radiat. Res.* **1995**, *144*, 251−7.
(39) Weiland, B.; Hüttermann, J. *Int. J. Radiat. Biol.* **1998**, *74*, 341−58.
(40) Wang, W.; Yan, M.; Becker, D.; Sevilla, M. D. *Radiat. Res.* **1994**, *137*, 2−10.
(41) Cullis, P. M.; Malone, M. E.; Merson-Davies, L. A. *J. Am. Chem. Soc.* **1996**, *118*, 2775−2781.
(42) Candeias, L. P.; Steenken, S. *Chem. Eur. J.* **2000**, *6*, 475−484.
(43) Kim, S.-H.; Rich, A. *J. Mol. Biol.* **1969**, *42*, 87−95.
(44) Close, D. M.; Nelson, W. H.; Bernhard, W. A. In *Proceedings of the Ninth International Congress of Radiation Research*; Chapman, J. D., Dewey, W. C., Whitmore, G. F., Eds.; Academic Press: San Diego, CA, 1991; p 396.
(45) Farley, R. A.; Bernhard, W. A. *Radiat. Res.* **1975**, *61*, 47−54.
(46) Bernhard, W. A. *Adv. Radiat. Biol.* **1981**, *9*, 199−280.
(47) Bernhard, W. A.; Hüttermann, J.; Close, D. M. *Radiat. Res.* **1987**, *112*, 54−61.
(48) Bernhard, W. A.; Mercer, K. R. *J. Phys. Chem.* **1987**, *91*, 6592−5.
(49) Box, H. C. *Top. Mol. Organ. Eng.* **1991**, *6*, 409−26.
(50) Close, D. M.; Bernhard, W. A. *J. Chem. Phys.* **1979**, *70*, 210−215.
(51) Close, D. M.; Hole, E. O.; Sagstuen, E.; Nelson, W. H. *J. Phys. Chem. A* **1998**, *102*, 6737−6744.
(52) Nelson, W. H.; Sagstuen, E.; Hole, E. O.; Close, D. M. *Radiat. Res.* **1992**, *131*, 10−17.
(53) Shui, X.; McFail-Isom, L.; Hu, G. G.; Williams, L. D. *Biochemistry* **1998**, *37*, 8341−8355.
(54) Goodsell, D. G.; Grzeskowiak, K.; Dickerson, R. E. *Biochemistry* **1995**, *34*, 1022−1029.
(55) Privé, G. G.; Yanagi, K.; Dickerson, R. E. *J. Mol. Biol.* **1991**, *217*, 177−199.
(56) Wahl, M.; Rao, S.; Sundaralingam, M. *Biophys. J.* **1996**, *70*, 2857−2866.
(57) Ramakrishnan, B.; Sundaralingam, M. *Biochemistry* **1993**, *32*, 11458−68.
(58) Ban, C.; Sundaralingam, M. *Biophys. J.* **1996**, *71*, 1222−1227.
(59) Bingman, C.; Li, X.; Zon, G.; Sundaralingam, M. *Biochemistry* **1992**, *31*, 12803−12812.
(60) Tippin, D. B.; Sundaralingam, M. *Acta Crystallogr. D* **1996**, *52*, 997−1003.
(61) Sadasivan, C.; Gautham, N. *J. Mol. Biol.* **1995**, *248*, 918−930.
(62) Wang, A.; Quigley, G.; Kolpak, F.; Crawford, J.; van Boom, J.; van der Marel, G.; Rich, A. *Nature* **1979**, *282*, 680−686.
(63) Gessner, R. V.; Frederick, C. A.; Quigley, G. J.; Rich, A.; Wang, A. H.-J. *J. Biol. Chem.* **1989**, *264*, 7921−7935.
(64) Egli, M.; Williams, L. D.; Gao, Q.; Rich, A. *Biochemistry* **1991**, *30*, 11388−11402.
(65) Crawford, J. L.; Kolpak, F. J.; Wang, A.; Quigley, G.; van Boom, J.; van der Marel, G.; Rich, A. *Proc. Natl. Acad. Sci. U.S.A.* **1980**, *77*, 4016−4020.
(66) Gatehouse, B. M.; Poppleton, B. J. *Acta Crystallogr. B* **1970**, *26*, 1761−1765.
(67) Viswamitra, M. A.; Reddy, B. S.; Lin, G. H.-Y.; Sundaralingam, M. *J. Am. Chem. Soc.* **1971**, *93*, 4565−4573.
(68) Bernhard, W. A.; Barnes, J.; Mercer, K. R.; Mroczka, N. *Radiat. Res.* **1994**, *140*, 199−214.